THERMO-HYDRAULIC PERFORMANCE EVALUATION OF HEAT EXCHANGER TUBE WITH VORTEX GENERATOR INSERTS

by

Ibtisam A. HASAN**, Wafa MAKI, and Yaser Ali ENAYA

Department of Electromechanical Engineering, University of Technology, Baghdad, Iraq

Original scientific paper
https://doi.org/10.2298/TSCI210528289H

This work is undertaken as a scientific experiment to test a new design of a turbulent generator. The current research experiments the influence of novel vortex generator inserts on heat transfers within a tube under a uniform heat flux. A Cu tube with a 45 mm inner diameter and 1350 mm length is used along with a solid disc injector (swirl generator) that comprises ten crescent holes with equal circumferential distribution angles around the disk canter. Subsequently, a swirl flow is generated by deviating the stream flow 45° causing it to spin in the direction of the axial flow. Flow directors are on 45^o angles toward the axial direction for each of the crescent holes. This study is an example of flow degradation. Reynolds numbers range from 6000 to 13500. Therefore, fluid-flow is treated as a turbulent system. All experiments done with air are regarded as a power fluid and Prandtl number is fixed at about 0.71. Thermo-hydraulic performance of heat exchanger is analyzed. The average heat transfer Nusselt number is calculated and discussed. The experiment found out that Nusselt number increases with an increase in Reynolds number as well as the number of swirl generators. At four vortex generators, the maximum augmentation in heat transfer is around 4.3 times greater than the plain tube and friction factor is about 1.28 with 5 vortex generators insets. The results indicate a promising heat exchanger enhancement in the local petroleum industries.

Key words: *thermo-hydraulic, heat exchanger, vortex generators*

Introduction

Over many decades, designers have attempted to build energy-saving and compact heat exchangers [1]. One way to approach this aim is by intensifying heat transfers by way of conveying. During the process of power fluid-flow at heat exchange, the boosting of heat transfer rate requires specific actions to decrease the laminar sub-layer thickness that is formed on the inner surface of the conduit. Generally, the techniques for enhancing heat transfer minimize the thermal resistance either by increasing the effective surface area of heat transfer or by generating turbulence insides the flow. Some previous studies have covered the methods that increase the affected areas for heat transfer as using extended surfaces [1, 2] or rough surfaces [3] that affect the boundary-layer state. The other option for enhancing heat exchanger thermal performance includes the insertion of geometry elements that boost local turbulence. The usage of these elements is restricted by the pressure drop. Flow turbulization is done by introducing elements to create an artificial turbulization to hinder the fluid path.

* Corresponding author, e-mail: Ibtisam.a.hasan@uotechnology.edu.iq

These disturbances increase heat transfer. Then, the pressure drop affects the friction factor that is important to manage the pressure drop. These changes are accompanied typically by a rise in pumping power that may lead to an increase in cost. Many investigations on the effects of various insertion types to induce turbulence have been conducted by placing an obstacle to the fluid-flow or by installing an injector in the flow pipe at defined points along the flow axis [4-7]. The decaying swirl flow can be created using various techniques. These are either active or passive. Swirl flow has several applications in the mechanical and chemical engineering field like separating and mixing devices, turbomachinery, combustion chambers, and chemical reactors [8]. Further, a conical injector has been inserted to generate a decaying swirl flow in the pipe to define its effect on heat and exergy transfer in a turbulent flow regime experimentally [9].

Another experiment on the generation of swirl flow was conducted by using shortened helical tape fixed at the entry of the test section [10]. The effects of inserting an axial vane inside heat exchanger tube for generating a swirl flow has also been studied [11]. Jafari *et al.* [12] has designed a swirling flow generator consisting of four holes as a star cross-section in a disk with several disks inserted along the axial direction of the tube to investigate their effects on the overall heat exchanger performance. The effects of the number of vanes in a propeller and its axial positions, besides the vane inclination angle with a vertical axis of the turbulence device technique in swirl generation, have been studied too [13]. Improved numerical shell and tube heat exchanger hydrodynamic characteristics resulted by using baffle type vortex generators (VG) [14]. Other research presented the effects of different baffle angles on heat transfer enhancement [15]. Exergy analysis is one of the methods which have been used to determine the optimum geometry of the propeller [16]. While others used a flat tape with various geometries [17], and many more utilized nanofluid to enhance the performance of heat exchanger [18-20].

The current study, however, offers novel swirl generator (SG) inserts. A disc consisting of ten crescent holes with equal circumferential distribution angles around the disk center. A decaying swirl flow was generated by deviating the stream flow 45°, which caused it to twirl around the axial flow direction. This was compared with the other SG devices used in heat exchangers customarily. This research focuses on the effects of the swirling generation insert numbers on the rate of convection along with the pressure drop inside the test tube (thermo-hydraulic performance). Meanwhile, the air was used as power fluid. Finally, the accuracy of results the plain tube outcomes are supported by available correlations of turbulent flows.

Experimental apparatus

Figure 1 shows a schematic diagram of the open loop system used in the experimental test. The experimental rig consists mainly of an inlet section (calming section), a test section with heating arrangement, and an air outfit system (blower). The main air outfit system equipment has a 6.5 kW blower motor, and a flow meter is employed to measure the flowrate. The test section included an aluminum tube with length, L = 1350 mm. Its diameters are inner, D_i = 45 mm and outer, D_o = 50 mm diameters, respectively. The tests are conducted under constant heat flux condition. The test tube is enveloped by an electrical heater to deliver a uniform and controlled heat flux. A variac controls the input electrical voltage to reach the desired power. The external surfaces of the test section are tightly insulated to reduce heat loss in the surroundings by radiation and convection. Heat losses are determined by measuring the temperatures at four various points at the outer surface of the thermal insulator by using *T*-type thermocouples. The axial heat losses are minimized at the test section by placing a Teflon layer in the inlet and outlet of the test tube.

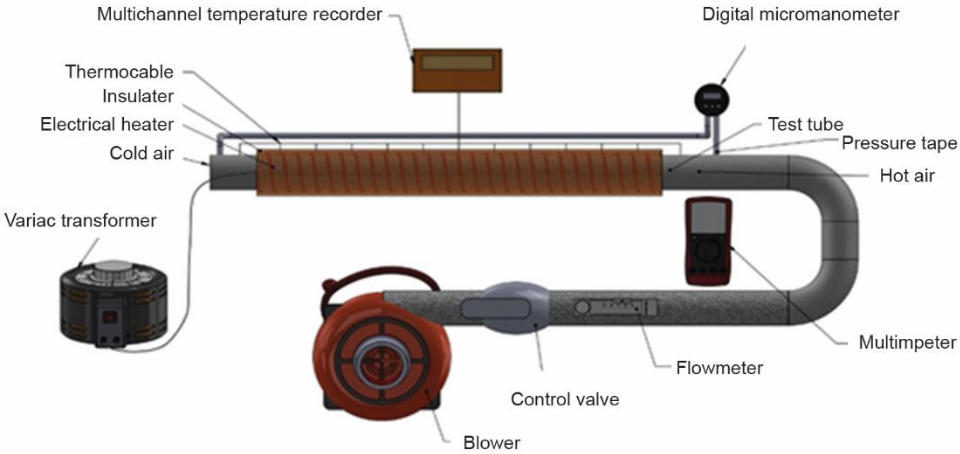

Figure 1. Experiment set-up schematic diagram

The temperature distribution along the outer surface wall of the test pipe is measured by fixing teen thermocouples at various points. The temperature of the test tube's main wall is determined by calculating the reading of ten distribution thermocouples. In order to measure the bulk temperatures of air, a thermocouple is fixed at the test section inlet along with other two thermocouples fixed at the test section outlet. To record the temperature of the test section, a multi-channeled temperature recorder with *T*-type thermocouple (calibrated) is used. The pressure drop across the test section is measured by a digital micromanometer through taps located at entrance and exit of the test section. Figure 2 shows the test tube details with the arrangement of the swirling VG insert.

Figure 2(a) shows a plain tube and the location of the single SG, with a relative spacing $S = L/2$. The other tubes contain different relative spacings, S/L, which are $S = L/3$, $L/4$, $L/5$, and $L/6$ for inserting 2, 3, 4, and 5 SG, respectively. To fix the swirl VG, teflon rings are attached to the inserts.

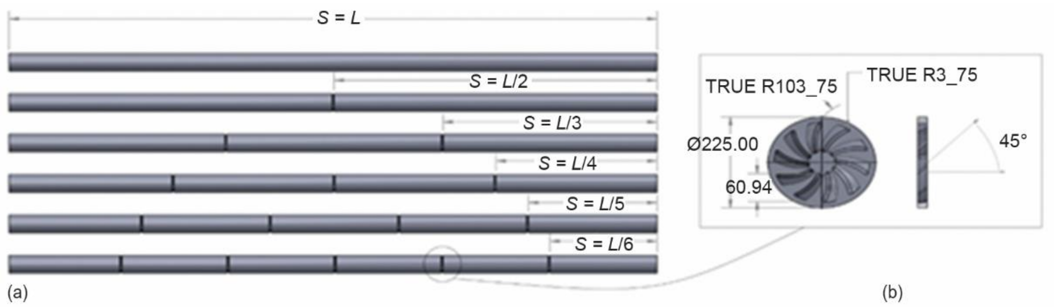

Figure 2. (a) Distribution of SG devices inserts and (b) a schematic diagram of a SG

The SG elements are illustrated with reference in fig. 2(b). It is consisting of ten similar crescent holes with equal circumferential distribution angle of 36° around the disk center. The cutting line of the crescent hole breaches the disk surface at an inclination angle of

Figure 3. Physical behavior of fluid-flow

45°. As soon as the fluid enters the SG device, it starts to spin in a swirl around the main direction of fluid-flow. Figure 3 demonstrates the default physical behavior of the fluid-flow.

The SG devices are designed and constructed by 3-D printing machines. The best quality available is used in printing the swirl devices and the used material is polylactic acid. The surfaces of the SG are treated for smoothness to reduce the friction losses.

Data reduction

Experimentally, six different values of Reynolds numbers (6000, 7500, 9000, 10500, 12000, and 13500), which are the generally used range in the local petroleum industries, are examined to show the effects of applying swirl flow on the overall performance of the heat exchanger. Currently, the air is used as a power fluid to flow through the insulated tube under uniform heat flux condition. The net thermal energy input, Q_1, to the air from the inner surface of the tube is determined while the electrical energy is supplied to the system:

$$Q_1 = VI - Q_{\text{losses}} \tag{1}$$

where V is the voltage and I – the current.

In the case of steady-state condition, the rate of heat, Q_2, transferred to air is expressed:

$$Q_2 = mC_p(T_{\text{bo}} - T_{\text{bi}}) \tag{2}$$

where T_{bo} and T_{bi} represent the fluid bulk temperatures at the inlet and the outlet, respectively.

The energy equilibrium test between heat losses due to the radiation and convection from the test section has shown that the applied electrical power on the test section 0.8-2.6% was greater than the heat absorbed by the fluid. The losses can be ignored as long as they are less than 5% [12], and the average of Q_1 and Q_2 are considered as an input heat to the air:

$$Q_{\text{average}} = \frac{Q_1 + Q_2}{2} \tag{3}$$

The convective heat transfer from inner surface of the tube is equal to the gained heat by air inside it. Therefore, the given energy balance equations are:

$$Q_{\text{air}} = \dot{m}C_p(T_{\text{bo}} - T_{\text{bi}}) = Q_{\text{conv.}} = \bar{h}A(\overline{T_{\text{w}}} - \overline{T_{\text{b}}}) \tag{4}$$

$$\overline{T_{\text{w}}} = \frac{\sum_{i=l}^{10} T_{\text{wi}}}{18} \text{ and } \overline{T_b} = \frac{T_{\text{bo}} + T_{\text{bi}}}{2}$$

where $\overline{T_{\text{b}}}$ and $\overline{T_{\text{w}}}$ [K] represent the air bulk and wall temperatures of the test tube, respectively. While $\bar{h}$ [Wm^{2}K^{-1}] is the average heat transfer coefficient. Then:

$$\bar{h} = \dot{m}C_p \frac{T_{\text{bo}} - T_{\text{bi}}}{A(\overline{T_{\text{w}}} - \overline{T_{\text{b}}})} \tag{5}$$

Define the mean Nusselt number as $\overline{\text{Nu}} = \bar{h}D/k$ and Reynolds number as $\text{Re} = \rho VD/\mu$.

Friction factor is defined:

$$f = \frac{\Delta P}{\frac{L}{D}\frac{\rho U^2}{2}} \tag{6}$$

where U [ms^{-1}] is the velocity of flow and ΔP – the pressure drop through the test tube.

The properties of thermal fluids are calculated at the bulk temperature while thermal performance factor, η, at same pumping power is [5]:

$$\eta = \frac{h_t}{h_p}\Big| pp = \frac{\dfrac{\mathrm{Nu}_t}{\mathrm{Nu}_p}}{\left(\dfrac{f_t}{f_p}\right)^{1/3}} \tag{7}$$

The Colburn *j*-factor is determined by using the relation attained among Reynolds, Prandtl, and Nusselt numbers [21].

$$j = \frac{\mathrm{Nu}}{\mathrm{Re}\,\mathrm{Pr}^{0.33}} \tag{8}$$

Uncertainty analysis

The experiment show there has been a possible error between the measured and the actual parameters for all laboratory experiments. Although the calibration, confirmation, and other experimental steps of the system aimed to improve the reliability of outcomes, the study of uncertainty was a critical step in minimizing the distance between the results and the reality. The research used the Moffat [22] approach for an analysis uncertainty of the independent variables and their effects. The variable value, XX, is considered a summary of the measured value, XX_{measured}, and a specific uncertainty is:

$$(\pm\delta XX): XX = XX_{\text{measured}} \pm \delta XX \tag{9}$$

The uncertainty value for a parameter is considered as a function of all the independent parameters:

$$[\varphi = \varphi(XX_1, \ldots, XX_n)] \text{ So: } \delta\varphi = \sqrt{\sum_{i=1}^{n}\left(\frac{\partial\varphi}{\partial XX_i}\delta XX_i\right)^2} \tag{10}$$

In this regard, the results of uncertainty for the friction factor and the Nusselt number are roughly 4% and 6%, respectively. In addition, the other measured parameters have relative variance of less than 4%, which is a reasonable value that satisfies the proper uncertainty and precision of instruments.

Results and discussion

Verification of experiment results

A smooth tube is examined, and measurements are estimated and compared to the relationship suggested by Dittus and Boelter for Nusselt number and Blasius for friction factor correlation [23].

$$\text{Dittus and Boelter correlation} \;\; \mathrm{Nu} = 0.023\mathrm{Re}^{0.8}\,\mathrm{Pr}^{0.33} \tag{11}$$

$$\text{Blasius correlation} \;\; f = 0.3164\,\mathrm{Re}^{-0.25} \tag{12}$$

A comparison between the recorded parameters and Dittus and Boelter correlation is illustrated in fig. 4. In order to get values within an acceptable range, the agreement between the interactions and the datasets reported is observed. The data is derived from the smooth tube studies of the proposed correlations (3.9% and 3.2%) representing the Nusselt number and *f*, respectively. This small de*via*tion in the experimental results allows experimentation to continue.

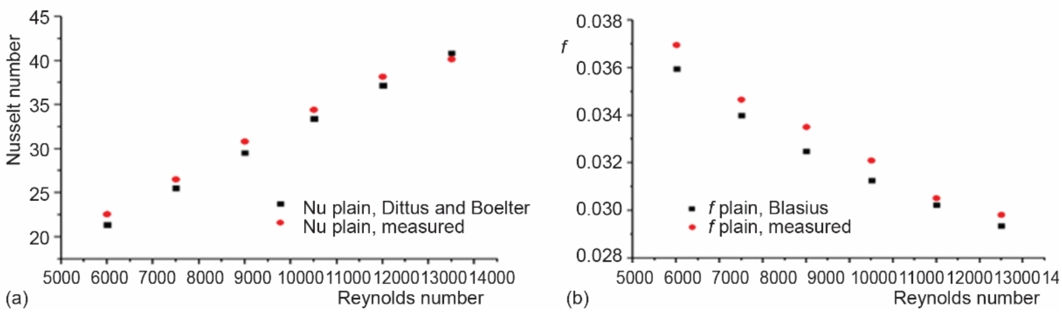

Figure 4. (a) **Nusselt number *vs.* Reynolds number for plain tube and (b) friction factor *vs.* Reynolds number for plain tube**

Axial temperature distribution

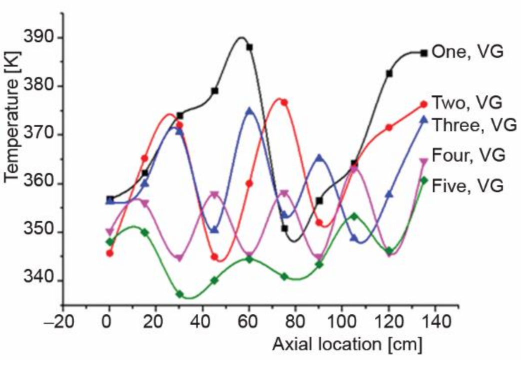

Figure 5. Axial distribution of tube surface temperature at Re = 9000 and different VG numbers

Figure 5 depicts the temperature distribution along the tube axes for various numbers of VG, at Reynolds number equal to 9000. The figure shows that the values of temperature increase along the tube length. The temperature decreases whenever a set of VG is inserted into the test tube. Air turbulent starts to increase when VG are inserted, which affect temperature distribution along the test tube. The best temperature decrease is achieved with 5-piece ($S = L/6$) of inserted VG which is close to 4-piece ($S = L/5$) of VG, that leads to include spacing and a high level of turbulent of a specific number of VG. Figures 6(a) and 6(b) shows the effects of different Reynolds numbers on the tube surface temperature with one VG ($S = L/2$) as shown in figs. 6(a) and 6(b) that illustrate the effects of four VG on $S = L/5$. In these figures, the effects of a number of VG inserts can easily be observed by following their line fig. 7(a) where the effects of insert numbers and flow rate vary from 6000 to 13500.

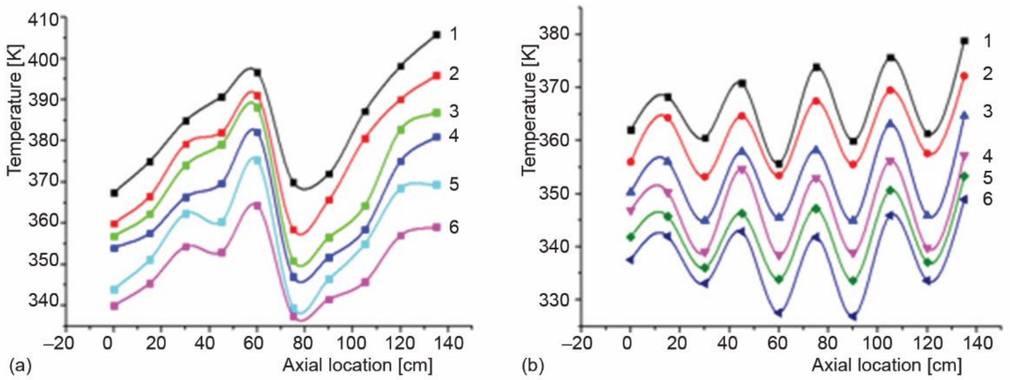

Figure 6. Axial distribution of tube surface temperature; (a) for one VG element and (b) for four VG elements; *1 – Re = 6000, 2 – Re = 7500, 3 – Re = 9000, 4 – Re = 10500, 5 – Re = 12000, 6 – Re = 13500*

Heat transfer characteristics

The main purpose of the experiments is to increase heat transfer comparing to smooth tube heat exchangers. Figures 7 and 8 show the outcome of all geometric inserts on the heat transfer. Figure 8 illustrates the experimental finding of Nusselt number with Reynolds number for a different number of VG along with a plain tube case. Nusselt number increases dramatically with the increase in Reynolds number suggesting an increase in convective mode of heat transfer. In addition, fig. 7 shows that the VG have the highest output while the smooth straight tube has the weakest performing point with the lowest Nusselt number. It is noticed that as the VG number increase, the heat transfer increases significantly. These dominant disruptions cause the generation of eddy and vortex near the VG, which cause the proper mixing of the flow stream that results in an increase in the frequency of eddy generation through VG, leading to an increase in heat transfer as well. These dominant disturbances can easily be seen in fig. 7. This tends to conclude that the rate of energy transfer increases with an increase in the VG number. The explanation is that VG inserts induce swirl flow/secondary flow and increased pressure gradient along the radial direction. The maximum increase in heat transfer is observed on four VG, which is approximately 4.3 times higher than

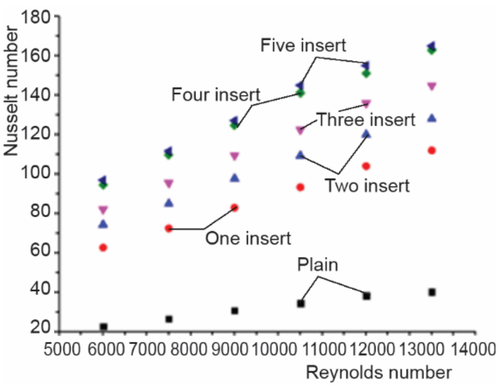

Figure 7. Nusselt number as a function of Reynolds number

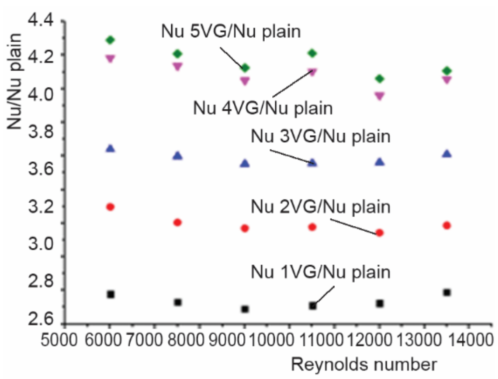

Figure 8. Heat transfer enhancement as a function of Reynolds number

for a plain tube at Reynolds number equal to 6000, as seen in fig. 8. The VG with 4 and 5 inserts have similar performance in the range of the current used Reynolds number, which indicates that four inserts may arrive at the saturated effect as will be seen in the performance evaluation, while the one VG insert has minimum Nusselt number.

Fluid-flow characteristics

The experimental findings for the friction factor are shown in fig. 9. This table defines experimental values for various numbers of VG and Reynolds number. For a particular case, friction factors usually decreases with the increasing Reynolds number as seen in fig. 9. The diagram indicates that differences in friction factors have a close relationship with both inserts and non-inserts tubes. Friction factor in tube cases with inserted VG is consistently greater than the plain tube as seen in fig. 9, which is explained through the use of VG, which contributes to more losses near boundary zones, resulting in a greater swirl flow with a longer period in the tube. Five VG have the highest friction. One VG has a minimum pressure, which decreases due to a minor disruption in the flow field that happens before and after the production of the vortex. The obtained frication factor results had similar trend as that cited in reference [7].

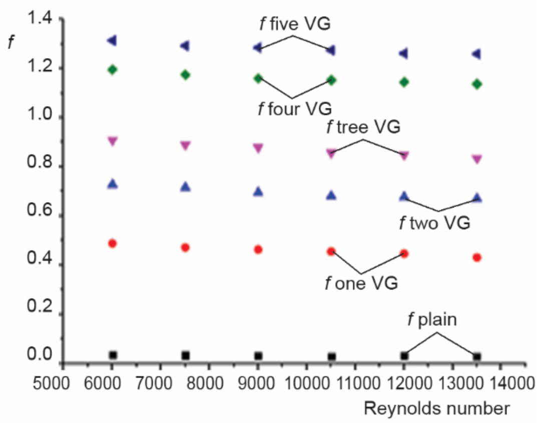

Figure 9. Friction factor as a function of Reynolds number

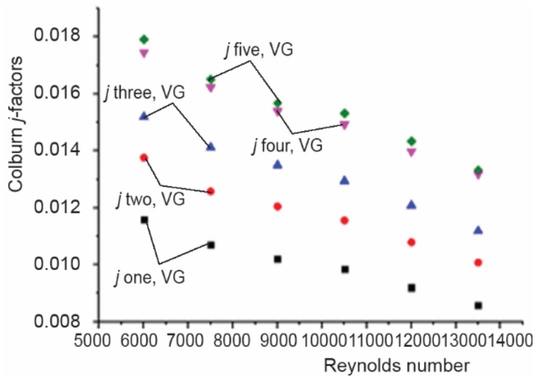

Figure 10. Colburn *j*-factors as a function of Reynolds number

Colburn j-factors

The findings of the study are used to measure *j*-factors for different configurations. As shown in fig. 10, the *j*-factors are plotted against the Reynolds number, with a comparative plot of plain tube output under the same condition. From fig. 10, it is concluded that *j*-factors improve the output over the increase of the VG number up to four VG element, which obtain similar results for the 5 VG element. The results of the increase in radial swirl flow, lead to an increase in longitudinal flow that increases the efficiency. It is also clear that the performance improvement of these inserts is considerably higher. As shown in fig. 10, the *j*-factors are planned against the Reynolds number, with a comparative plan for a smooth tube output under the same condition, it is concluded that *j*-factors improve the output over the increase of the VG number up to four VG element, which obtain similar results for the 5 VG element. The results of the increase in radial swirl flow, lead to an increase in longitudinal flow that increases the efficiency. It is also clear that the performance improvement of these inserts is considerably higher.

Performance evaluation

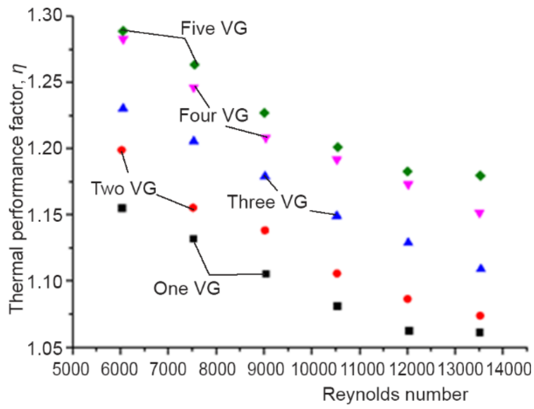

Figure 11. Thermal performance factor, η, as a function of Reynolds number

Turbulence generated by VG inserts is more beneficial in terms of heat transfer compared to frictional losses. As increase in heat transfer is simultaneously followed by a pressure reaction, the performance factor, η, is employed as an effective measure to determine the practical feasibility between the insertion of the VG and the plain tube. These outcomes in a combined evaluative parameter take into account heat transfer efficiency and pressure penalties as the difference of the η with the Reynolds number can be seen in fig. 11. It should be noted that the performance of the inserts generally increase in all different situations, leading to a consistent increase in performance. Therefore, inserts with varying degrees of improvement have never shown to be detrimental to the transfer of energy compared to tubes with smooth or flat cross-sections. Performance coefficient values higher than unity suggests improvement because the turbulence is much more than the decrease in performance due to frictional losses. The performances of insert distribution cases is quite similar so that their curves in fig. 11 are approximately the same. Figure 11 shows that the four VG in the tube show the greatest thermal enhancement efficiency all over the studied Reynolds number range and the greatest performance parameter approximate 1.29, at Reynolds number equal to 6000. Besides, it can be seen from fig. 11 that the five VG performance insertion case is smaller comparing to four VG, but rather closer.

Comparison with previous works

As per the experimental analysis, a very considerable increase in thermal efficiency factor and heat transfer can be noted when VG are used as an insert geometry. Table 1 shows a comparison of the current work with some related past work, which their data is taken from the original references. There are several benefits of using VG over other types of inserts. It is quite simple to produce VG since they are made by using a punching and blanking process where specific sizes of a die and a punch are used. The cost of production is much lower, as only one process is employed in the production of VG. They are not expensive compared to conical rings or twisted tapes. Manufacturing other insert geometries, such as twisted tape has further challenges as there's all the time a possibility of material wastage, as twist ratios should be preserved equally in the twisted tape. The use of VG can therefore be beneficial compared with other geometries employed in this type of analysis.

Table 1. The present results comparison with past studies

Reference	Nu/Nu plain tube	Overall efficiency
[24]	4.5	1.42
[25]	6.5	1.54
[26]	4.1	1.1
[27]	3.3	1.8
[7]	4.45	1.4
Present work	4.3	1.29

Conclusion

This experimental study shows the finding of friction factor, Nusselt number, and thermal efficiency factor characteristics for flow in a circular tube with VG inserts in a turbulent flow control. The VG with various numbers of insertions have also been examined. Nusselt number and friction factor values are greater than plain smooth tube over the entire range of geometric and flow parameters. Maximum heat transfer improvement is noticed in the case of insertion of four VG. Thermo-hydraulic efficiency is roughly more than uniform in all situations, suggesting an effect of the increase in heat transfer because the increase of the augmentation apparatus is more prevalent than the result of the increase in friction reactions/penalty. Thermohydraulic output of four VG (maximum value) is 12.7% higher than one VG (minimum value) at Re = 6000.

From tab. 1, it can be concluded, that the present work's efficiency and Nu/Nu plain tube are in the same range and close to the other works. Besides, the present work is manufacturally more facilitating than the previous works, especially in the local petroleum industries.

This research has shown to be valuable for the design of heat exchanger tubes, as it improved thermal efficiency, which ultimately contributes to the system compactness.

References

[1] Meyer, J. P., Olivier, J.A., Transitional Flow Inside Enhanced Tubes for Fully Developed and Developing Flowwith Different Types of Inlet Disturbances: Part I – Adiabatic Pressure Drops, *Int. J. Heat Mass Transf., 54* (2011), 7, pp. 1587-1597
[2] Sadeghzadeh, H., *et al*., Optimization of a Finned Shell and Tube Heat Exchanger Using a Multi-Objective Optimization Genetic Algorithm, *Sustainability, 7* (2015), 9, pp. 11679-11695
[3] Attalla, M., Maghrabie, H., An Experimental Study on Heat Transfer and Fluid-flow of Rough Plate Heat Exchanger Using Al_2O_3/Water Nanofluid, *Exp. Heat Transf., 33* (2020), 3, pp. 261-281
[4] Salih, I., Thermal Characterization of Turbulent Flow in a Tube With Discrete Coiled Wire Insert, *J. Eng. Dev., 18* (2017), 1, pp. 1-12
[5] Al-Obaidi, A., Sharif, A., Investigation of the Three-Dimensional Structure, Pressure Drop, and Heat Transfer Characteristics of the Thermohydraulic Flow in a Circular Pipe with Different Twisted-Tape Geometrical Configurations, *J. Therm. Anal. Calorim., 143* (2021), 5, pp. 3533-3558
[6] Samruaisin, P., Effect of Sparsely Placed Twisted Tapes Installed with Multiple-Transverse Twisted-Baffles on Heat Transfer Enhancement, *J. Therm. Anal. Calorim., 140* (2020), 3, pp. 1159-1175
[7] Kuma, A., *et al*., Experimental Investigation on Thermal Performance and Fluid-flow Characteristics in Heat Exchanger Tube with Solid Hollow Circular Disk Inserts, *Appl. Therm. Eng., 100* (2018), May, pp. 227-236
[8] Sheikholeslami, M., Review of Heat Transfer Enhancement Methods: Focus on Passive Methods Using Swirl Flow Devices, *Renew. Sustain. Energy Rev., 49* (2015), Sept., pp. 444-469
[9] İrfan, K., F., *et al*., Effect of Swirl Generator Inserted Into a Tube on Exergy Transfer: Decaying Flow, *Exp. Heat Transf., 27* (2014), 5, pp. 472-487
[10] Gül, H., Heat Transfer Enhancement in Circular Tubes Using Helical Swirl Generator Insert at the Entrance, *Int. J. Therm. Sci., 46* (2007), 12, pp. 1297-1303
[11] Ahmadvand, M.,*et al*., An Experimental Study and CFD Analysis Towards Heat Transfer and Fluid-flow Characteristics of Decaying Swirl Pipe Flow Generated by Axial Vanes, *Meccanica, 45* (2010), 1, pp. 111-129
[12] Jafari, M., *et al*., The Experimental Investigation Concerning the Heat Transfer Enhancement *Via* a Four-Point Star Swirl Generator in the Presence of Water-Ethylene Glycol Mixtures, *J Therm Anal Calorim, 144* (2021), Feb., pp. 167-178
[13] Bali, T., Ayhan, S., Exergy Analysis of Heat Transfer in a Turbulent Pipe Flow by a Decaying Swirl Generator, *Int. J. Exergy, 5* (2008), 1, pp. 64-77
[14] Menni, Y., *et al*., Enhancement of the Hydrodynamic Characteristics in Shell-and-Tube Heat Exchangers by Using W-Baffle Vortex Generators, *Period. Polytech. Mech. Eng., 64* (2020), 3, pp. 212-223

[15] Ameur, H., Effect of Corrugated Baffles on the Flow and Thermal Fields in a Channel Heat Exchanger, *J. Appl. Comput. Mech.*, *6* (2020), 2, pp. 209-218
[16] Chavda, N., Parekh, P., Experimental and Exergy Analysis of a Double Pipe Heat Exchanger for Parallel Flow Arrangement, *J. Eng. Res. Appl.*, *4* (2014), 7, pp. 09-13
[17] Sivasubramaniam, A. P., *et al*., Heat Transfer and Friction Factor Characteristics of Pipe-in-Pipe Heat Exchanger Fitted with Variant Plain Tape Insert, *Thermal Science*, *24* (2020), 1B, pp. 623-633
[18] Jasim, Q., Improving Thermal Performance Using AL_2O_3-Water Nanoflouid in a Double Pipe Heat Exchanger Filling with Porous Medium, *Thermal Science, 24* (2020), 6B, pp. 4267-4275
[19] Sözen, A., *et al.*, The Heat Transfer Enhancement of Concurrent Flow and Counter Current Flow Concentric Tube Heat Exchangers by Using Hexagonal Boron Nitride-Water Nanofluid, *Thermal Science, 23* (2019), 6B, pp. 3917-3928
[20] Haghshenasfard, M., *et al*., Numerical and Experimental Investigation of Heat Transfer of ZnO/Water Nanoflouid in the Concentric Tube and Plate Heat Exchangers, *Thermal Science, 15* (2011), 1, pp. 183-194
[21] Meyer, J., Olivier, J. A., Transitional Flow Inside Enhanced Tubes for Fully Developed and Developing Flow with Different Types of Inlet Disturbances: Part I - Adiabatic Pressure Drops, *Int. J. Heat Mass Transf., 54* (2011), 7, pp. 1587-1597
[22] Moffat, R. J., Describing the Uncertainties in Experimental Results, *Exp. Therm. Fluid Sci., 1* (1988), 1, pp 3-17
[23] Shah, R., Sekulic, D., *Fundamentals of Heat Exchanger Design*, John Wiley and Sons Inc., New York, USA, 2003
[24] Eiamsa-Ard, S., *et al*., Thermohydraulics of Turbulent Flow Through Heat Exchanger Tubes Fitted with Circular-Rings and Twisted Tapes, *Chinese J. Chem. Eng., 21* (2013), 6, pp. 585-593
[25] Promvonge, P., Thermal Augmentation in Circular Tube with Twisted Tape and Wire Coil Turbulators, *Energy Convers. Manag., 49* (2008), 11, pp. 2949-2955
[26] Promvonge, P., Eiamsa-Ard, S., Heat Transfer in a Circular Tube Fitted with Free-Spacing Snail Entry and Conical-Nozzle Turbulators, *Int. Commun. Heat Mass Transf., 34* (2007), 7, pp. 838-848
[27] Promvonge, P., Heat Transfer Behaviors in Round Tube with Conical Ring Inserts, *Energy Convers, 1* (2008), 49, pp. 8-15

Paper submitted: May 8 2021
Paper revised: August 13, 2021
Paper accepted: August 19, 2021